

Phonon-confinement effect on electron energy loss in one-dimensional quantum wires

V. B. Campos* and S. Das Sarma

Joint Program for Advanced Electronic Materials, Department of Physics, University of Maryland, College Park, Maryland 20742

M. A. Stroschio

U.S. Army Research Office, P.O. Box 12211, Research Triangle Park, North Carolina 27709

(Received 12 November 1991; revised manuscript received 29 April 1992)

We calculate, within the electron-temperature model, hot-electron intrasubband energy relaxation rates via LO-phonon emission in GaAs quantum wires, taking into account quantum degeneracy, dynamical screening, hot-phonon bottleneck, and, in particular, phonon confinement. Two prevailing macroscopic models of phonon confinement, namely, the slab or the electrostatic model and the guided or the mechanical model, are compared quantitatively. We find that the slab model, while giving relaxation rates comparable to the bulk-phonon emission rates, leads to an order of magnitude faster relaxation than the guided model. For reasonable parameter values, the hot-phonon-bottleneck effect is found to be the single most important physical mechanism determining energy relaxation. Numerical values for electronic-energy-loss rates in GaAs quantum wires are provided for both models of phonon confinement for a range of values of the relevant parameters, including confinement size, carrier density, hot-phonon lifetime, and electron temperature.

In order to obtain a realistic estimate for the energy-loss rate due to LO-phonon emission from a hot-electron gas in quasi-one-dimensional quantum wire structures, the effect of the confinement of the phonon mode should be taken into account, particularly in narrower wires. Phonon confinement causes changes in the selection rules for transitions involving subband electrons and also affects the magnitude of the electron-phonon interaction matrix element, consequently modifying the hot-electron energy relaxation rate compared with the bulk-phonon emission case.

Considerable work has recently been done¹⁻³ on the role of confined phonon modes in the hot-electron relaxation phenomena in semiconductor quantum wells. It is now well accepted that in narrow quantum wells confined phonon modes play a quantitatively significant role¹⁻³ in determining the experimentally measured⁴ energy relaxation rates. Electron-confined LO-phonon interaction in quantum-well systems has been studied using two different macroscopic approaches to phonon confinement: the electrostatic or the slab modes¹ and the mechanical or the guided modes.² Although there has been some earlier work on hot-electron transport in quantum wires,⁵ only recently^{6,7} has the problem hot-electron energy loss in these systems been addressed. In this paper we provide a calculation of hot-electron energy relaxation in semiconductor quantum wires due to *confined* LO-phonon emission, taking into account quantum degeneracy, dynamical screening, and hot-phonon bottleneck. We compare the two existing macroscopic models of phonon confinement and compare them with the case of bulk-phonon emission (i.e., no phonon confinement). We neglect the interface phonon modes, which have exponentially decaying amplitudes into the wire—this is expected to be a good approximation for wires which are not too narrow.

Let us consider a quantum wire of rectangular cross section along the x axis, with finite y and z dimensions, given, respectively, by L_y and L_z . We assume that the walls are impenetrable; that is, the confining potential well is an infinite square well. We are interested in studying both the macroscopic approaches for phonon confinement. They differ essentially in the way the boundary conditions are applied. In the slab model one applies boundary conditions on the electrostatic potential whereas in the guided model it is the electric field which is made to vanish at the interfaces. Then, mathematically, within our approximation scheme (infinite barriers characterizing the interfaces), the difference between these two models is represented only by the interchange of the sine and cosine functions in the vibrational amplitudes of the modes.⁸

In the slab model, the vibrational amplitude is given by

$$u_{2s+1}(t) \propto \sin \left[(2s+1) \frac{\pi t}{L_t} \right], \quad (1)$$

$$u_{2s}(t) \propto \cos \left[2s \frac{\pi t}{L_t} \right], \quad (2)$$

where s is a positive integer, and $t=y,z$ corresponds to the confined direction. The modes corresponding to Eq. (1) are symmetric while Eq. (2) gives rise to antisymmetric modes. In the mechanically confined model, we use boundary conditions on the atomic displacements at the interfaces. The vibrational amplitudes of these guided modes are given by

$$u_{2s+1}(t) \propto \cos \left[(2s+1) \frac{\pi t}{L_t} \right], \quad (3)$$

$$u_{2s}(t) \propto \sin \left[2s \frac{\pi t}{L_t} \right]. \quad (4)$$

The one-dimensional Fröhlich Hamiltonian describing the interaction between an electron and confined LO-phonon modes can be written as

$$H_{1D} = 2\alpha' \sum_{k_x} e^{-ik_x x} \sum_{m=1}^{\infty} \sum_{n=1}^{\infty} \xi_m(y) \xi_n(z) \lambda_{mn} \beta_{mn}, \quad (5)$$

where

$$\lambda_{mn} = \left[k_x^2 + \left[\frac{m\pi}{L_y} \right]^2 + \left[\frac{n\pi}{L_z} \right]^2 \right]^{-1/2}, \quad (6)$$

and

$$\beta_{mn} = A_{mn}(k_x) + A_{mn}^\dagger(-k_x). \quad (7)$$

Here A (A^\dagger) is a linear combination of the annihilation (creation) operator for the phonons, defined by

$$\begin{aligned} A_{mn}(k_x) = & \frac{1}{2} [(-1)^{m+1} a(k_x, k_y, k_z) + a(k_x, k_y, -k_z) \\ & + (-1)^{n+m} a(k_x, -k_y, k_z) \\ & + (-1)^{n+1} a(k_x, -k_y, -k_z)]. \end{aligned} \quad (8)$$

The functions ξ_n , which are determined by the confinement mode, are defined as follows for the slab modes:

$$\xi_n(t) = \sin \left[n \frac{\pi t}{L_t} + \frac{\pi}{2} \delta_n \right], \quad (9)$$

and for the guided modes

$$\xi_n(t) = \cos \left[n \frac{\pi t}{L_t} + \frac{\pi}{2} \delta_n \right], \quad (10)$$

with $\delta_n = 1$ if $n = \text{odd}$, and $\delta_n = 0$ if $n = \text{even}$. The constant α' is defined in terms of the usual dimensionless bulk Fröhlich constant α as

$$\alpha' = \left[\frac{4\pi\alpha}{V} \right] \left[\frac{\hbar^2}{2m} \right]^{1/2} (\hbar\omega_{LO})^{3/2},$$

where $V = L_x L_y L_z$ is the three-dimensional volume, and we have assumed dispersionless LO-phonons of frequency ω_{LO} . The electrons are taken to be in an isotropic parabolic conduction band, defined by a band effective mass m^*

Assuming the extreme quantum limit (i.e., the electrons are confined to the lowest one-dimensional subband in the quantum wire) the electron-phonon interaction matrix element is given by (within the infinite square potential confinement model)

$$M_{mn}^2(q) = 2\alpha \left[\frac{\hbar^2}{2m^*} \right]^{1/2} (\hbar\omega_{LO})^{3/2} F_{mn}(q), \quad (11)$$

where $F_{mn}(q)$ is the appropriate form factor with m, n confined phonon mode indices,

$$F_{mn}(q) = \frac{32\pi}{L_y L_z} P_{mn}^2 \left[q^2 + \left[\frac{m\pi}{L_y} \right]^2 + \left[\frac{n\pi}{L_z} \right]^2 \right]^{-1/2}. \quad (12)$$

The quantity P_{mn} , the y - and z -dependent factor in the matrix element, is the overlap integral between the electronic ground-state wave function and the phonon confined mode, and, is given by

$$\begin{aligned} P_{mn} = & \left[\frac{2}{L_y} \right] \left[\frac{2}{L_z} \right] \\ & \times \int_{-L_y/2}^{L_y/2} dy \int_{-L_z/2}^{L_z/2} dz \cos^2 \left[\frac{\pi y}{L_y} \right] \cos^2 \left[\frac{\pi z}{L_z} \right] \\ & \times \xi_m(y) \xi_n(z), \end{aligned} \quad (13)$$

with the functions $\xi_m(t)$ defined by Eqs. (9) and (10). Since the nonvanishing integrals of the type above are those involving only products of cosines, the overlap integrals, for both confining modes, can be written as

$$P_{mn} = \frac{(8/\pi)^2}{mn(4-m^2)(4-n^2)} \sin \left[m \frac{\pi}{2} \right] \sin \left[n \frac{\pi}{2} \right]. \quad (14)$$

Due to the functional dependence of the phonon wave function in each confined case, in order for P_{mn} to be nonzero, we must have both m and n odd integers for the slab modes. The total matrix element is therefore obtained by performing the sum over these odd labels. The dominant contribution to this sum is made by the mode with $m = n = 1$, since it can be shown that $|P_{13}| = 0.2P_{11}$ and $|P_{ij}| \leq 0.04P_{11}$ for $i, j > 1$. Thus, in the slab model it constitutes a good approximation to consider only the mode $m = n = 1$. On the other hand, for the guided modes, where m and n must be all even, only the term $m = n = 2$ has a nonvanishing contribution to the matrix element. Thus, in both cases we can consider only one value for P , which corresponds to the lowest possible m and n for the given model.

Our goal is to calculate the energy loss per electron via intrasubband relaxation within the electron temperature model. Except for the phonon confinement, this calculation is similar to our earlier work⁷ on hot-electron energy relaxation via the bulk LO-phonon emission. We make the standard finite-temperature random-phase approximation (RPA) to describe⁹ the electronic response, and, use the kinetic approximation¹⁰ to incorporate the hot-phonon-bottleneck effect.

The power loss per carrier, for lattice temperatures much smaller than the electron temperature T , can be written as¹⁰

$$P = \frac{1}{N} \sum_q \int_0^\infty d\omega \hbar\omega n_T(\omega) \frac{R_q}{1 + \tau_{ph} R_q} \delta(\omega - \omega_q), \quad (15)$$

where the scattering rate R_q can be expressed in terms of the one-dimensional electron-phonon coupling strength M_q and the finite-temperature reducible polarizability⁹ for the one-dimensional electron gas $\chi(q, \omega)$ as

$$R_q = -\frac{2}{\hbar} M_q^2 \text{Im}\chi(q, \omega), \quad (16)$$

where ω_q is the phonon frequency and n_T is the Bose factor at the electron temperature T . In this formula, the effects of electron-electron interaction are included through the dynamically screened polarizability function. We consider electron temperatures low enough so that $k_B T \ll \hbar\omega_{\text{LO}} = \hbar\omega_q$, which allows us to consider only the one-phonon emission process. In Eq. (15) τ_{ph} is the empirical hot-phonon lifetime. The value of τ_{ph} is a measure of the probability of the emitted LO phonons to be reabsorbed by the hot-electron gas causing a phonon-bottleneck effect. For a low-density electron gas, at temperatures high enough so that the electrons are nondegenerate ($k_B T \gg E_F$), we could describe the system as obeying classical Maxwell-Boltzmann statistics. We refer to this as the classical model, and use it for comparison with our quantum results.

In the rest of the paper we present our numerical results for the intrasubband energy-loss rates in GaAs quantum wires, where we have used the following parameters: $m = 0.07m_e$, $\hbar\omega_{\text{LO}} = 36.8$ meV, $\alpha = 0.07$. We consider wires with lateral dimensions between 10 to 1000 Å, electron densities from 10^3 to 10^7 cm $^{-3}$, and electron temperatures between 50 and 300 K (the lattice temperature is taken to be zero). We include quantum degeneracy, finite-temperature dynamical screening, hot-phonon and phonon-confinement effects, but neglect phonon self-energy corrections (which are very small in one-dimensional systems) and interface phonons (which are negligible, except for very narrow wires).

In Fig. 1 we show the numerical results for the power loss as a function of the inverse of the electron temperature, for $L_y = L_z = 50$ Å and electron densities of 10^4 and 10^6 cm $^{-3}$. The solid curves correspond to the slab modes, while the dashed curves represent the mechanically guided modes. We present the curves corresponding to the unscreened system, as well as the dynamically screened results, obtained with and without the hot-phonon effect. In the scale of this figure, it is not possible to distinguish between the classical result and the results without screening for both models. Since the hot-phonon lifetime in GaAs quantum wires is not experimentally known, we have used $\tau_{\text{ph}} = 7$ ps which is the bulk experimental value.¹¹ One can see that the power loss has an exponential dependence on the inverse of the temperature with an exponent $\hbar\omega_{\text{LO}}/k_B T$. The preexponential factor can be written as $\hbar\omega_{\text{LO}}/\tau$, where τ is the electron-energy relaxation time, leading to $P \approx (\hbar\omega_{\text{LO}}/\tau) \exp(-\hbar\omega_{\text{LO}}/k_B T)$. These results show that the inclusion of the hot-phonon effect considerably lowers the energy-loss rate. This reduction is more pronounced for the slab modes where the energy-loss rate is larger.

In Fig. 2 we show the electronic relaxation time τ , as calculated from the power loss, as a function of the electron density for $L_y = L_z = 100$ Å and $\tau_{\text{ph}} = 0$ and 7 ps. The hot-phonon effect is significant even at low densities. For all densities and wire sizes, τ for the guided modes is much larger than that for the slab modes, indicating a much slower relaxation due to guided modes. Figure 3

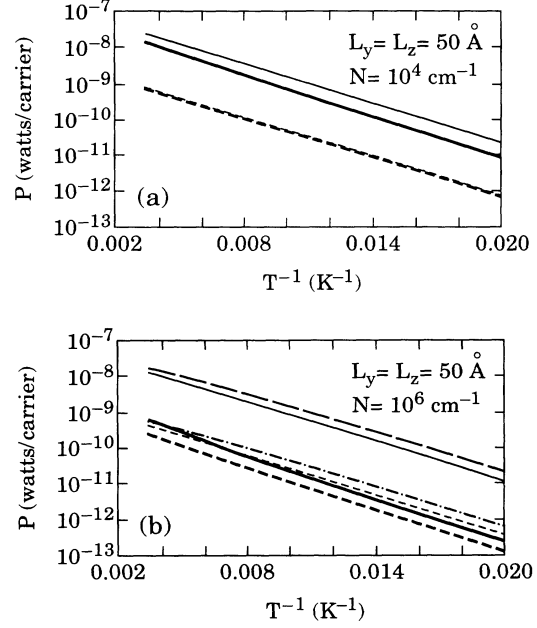


FIG. 1. Power loss per carrier as a function of inverse electron temperature for a quantum wire of lateral dimension $L_y = L_z = 50$ Å. We present the results for the slab phonon modes (solid curves) and the guided modes (dashed curves) for two electronic densities: (a) 10^4 cm $^{-3}$ and (b) 10^6 cm $^{-3}$. For both models the power loss is shown in the unscreened approximation, and with dynamical screening with hot-phonon effect, $\tau_{\text{ph}} = 7$ ps (thick lines) and $\tau_{\text{ph}} = 0$ (thin lines). For $N = 10^6$ cm $^{-3}$, the top long-dashed line represents the unscreened result for the slab model, and the dashed-dotted line for the guided model. For the low densities, the unscreened results coincide with the result for $\tau_{\text{ph}} = 0$ in the figures.

represents the dependence of the electronic relaxation time on the hot-phonon lifetime for both models and for the same wire parameters as before. There is a strong dependence on τ_{ph} particularly for larger values of the phonon lifetime. The overall behavior is the same for both models, but the guided modes produce τ which are about 20 times larger than that for the slab modes in the region of small values of τ_{ph} (≤ 0.5 ps). Our results based

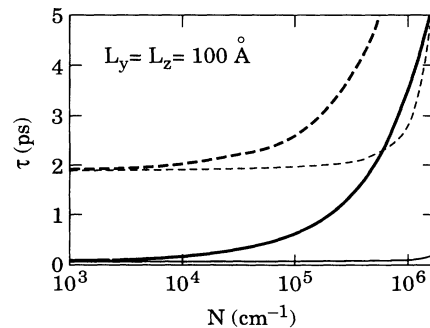


FIG. 2. Electron relaxation time τ as a function of the electron density for $L_y = L_z = 100$ Å, as obtained from the power loss, considering the slab phonon modes (solid curve) and the guided modes (dashed curve). The thin curves correspond to $\tau_{\text{ph}} = 0$ and the thick ones to $\tau_{\text{ph}} = 7$ ps.

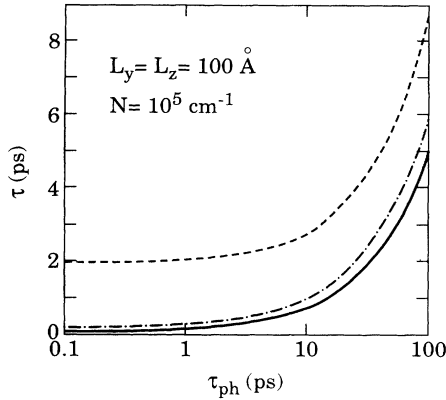


FIG. 3. Electron relaxation time τ as a function of the phonon lifetime τ_{ph} for a wire with $L_y=L_z=100 \text{ \AA}$ and $N=10^5 \text{ cm}^{-1}$ for the slab modes (solid curve) and the guided modes (dashed curve). We present also the bulk-phonon results (dashed-dotted curve) for comparison.

on the slab modes are close to those obtained⁷ using the bulk phonons whereas the guided-mode relaxation is substantially slower.

In Fig. 4 we show the electron relaxation time τ vs $L_y=L_z$, the lateral dimensions of the wire. The results correspond to both models of phonon confinement with electronic density of 10^5 cm^{-1} and $\tau_{\text{ph}}=0$ and 7 ps. The results for the guided modes are more strongly dependent on the dimensions of the wire, even when $\tau_{\text{ph}}=0$. For larger wires, the difference between the models is striking. In Fig. 5 we plot the wire size dependence of the ratio between the values of τ for the two confined-phonon models for a given τ_{ph} (solid curves) and the ratio between the results for the two values of phonon lifetimes for each model (dashed curves). As can be seen from the figure, the ratio of the relaxation rates for $\tau_{\text{ph}}=7 \text{ ps}$ and $\tau_{\text{ph}}=0 \text{ ps}$ is approximately a constant close to unity for the mechanical model. This implies that the inclusion of the hot-phonon effect does not drastically affect the size dependence of the energy relaxation in the mechanical model.

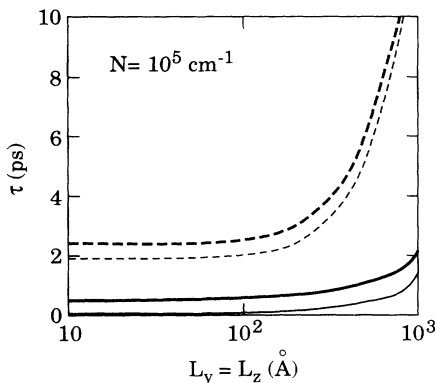


FIG. 4. Electron relaxation time τ as a function of the lateral dimension of the wire $L_y=L_z$ for electronic density $N=10^5 \text{ cm}^{-1}$. The solid lines represent the results for the slab modes and the dashed lines for the guided modes. We have used $\tau_{\text{ph}}=0$ (thin curves) and $\tau_{\text{ph}}=7 \text{ ps}$ (thick curves).

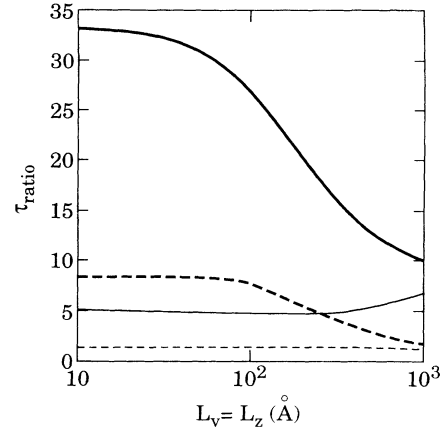


FIG. 5. Ratio of electron relaxation rates as a function of the lateral dimension of the wire for electronic density $N=10^5 \text{ cm}^{-1}$. The solid lines represent the ratio between the guided- and the slab-modes result, obtained considering dynamical screening and two different values for the phonon lifetime ($\tau_{\text{ph}}=0$ corresponds to the thick curve and $\tau_{\text{ph}}=7 \text{ ps}$ to the thin curve). The dashed lines represent the ratio of the electronic relaxation rates between the results obtained with hot phonons ($\tau_{\text{ph}}=7 \text{ ps}$) and those without hot phonons. The thick dashed curves correspond to the slab modes and the thin curves to the mechanically guided modes.

For the slab modes, however, the inclusion of finite τ_{ph} becomes very important in the narrower systems ($L_y=L_z \leq 300 \text{ \AA}$) and decreasingly important for systems with larger lateral dimensions. Without the hot-phonon correction the dependence of this ratio on the wire dimension is much stronger for narrower wires. In general, when τ_{ph} is much larger than τ calculated without hot-phonon correction (i.e., with $\tau_{\text{ph}}=0$), hot-phonon effects are extremely important whereas they are unimportant in the opposite situation.

In summary, we have calculated the hot-electron energy relaxation rate in GaAs quantum wires for intrasubband relaxation via confined LO-phonon mode emission in the electric quantum limit. Our calculation includes electron- and phonon-confinement effects, quantum degeneracy, dynamical screening, and the hot-phonon-bottleneck effect. We compare the two standard continuum phonon-confinement models, namely the slab and the guided-mode models, and find, consistent with the quantum-well situation, that the guided (mechanical) modes produce more than an order of magnitude slower energy relaxation than the slab (electrostatic) modes for intrasubband relaxation processes. Our slab results are close to the earlier calculated bulk results.⁷ The hot-phonon bottleneck is found to be the single most important physical mechanism in our calculations provided $\tau_{\text{ph}} \gtrsim 1 \text{ ps}$. Our calculated relaxation rates are comparable to those found in quantum wells.

This work was supported by the U.S. ARO and the U.S. ONR. V.B.C. also acknowledges support from FAPESP (Fundação de Amparo à Pesquisa do Estado de São Paulo, Brazil). S.D.S. thanks the Graduate Research Board of the University of Maryland for support.

*Permanent address: Departamento de Física, Universidade Federal de São Carlos, São Paulo, Brazil.

- ¹J. K. Jain and S. Das Sarma, *Phys. Rev. Lett.* **62**, 2305 (1989); K. Mori and T. Ando, *Phys. Rev. B* **40**, 6175 (1989); S. Rudin and T. L. Reinecke, *ibid.* **41**, 7713 (1990); L. Wendler and R. Pechsted, *Phys. Status Solidi B* **141**, 129 (1987).
- ²B. K. Ridley, *Phys. Rev. B* **39**, 5282 (1989); M. Babiker, *J. Phys. C* **16**, 683 (1986); B. K. Ridley and M. Babiker, *Phys. Rev. B* **43**, 9096 (1991).
- ³H. Rucker, E. Molinari, and P. Lugli, *Phys. Rev. B* **44**, 3463 (1991).
- ⁴A. Seilmair *et al.*, *Phys. Rev. Lett.* **59**, 1345 (1987); J. F. Ryan and M. Tatham, *Solid State Electron.* **32**, 1429 (1989), and references therein.
- ⁵See, for example, A. Ghosal *et al.*, *J. Appl. Phys.* **59**, 2511 (1986); S. Briggs *et al.*, *Phys. Rev. B* **38**, 8163 (1988); T. Yamada *et al.*, *ibid.* **40**, 6295 (1989).
- ⁶S. Das Sarma, V. B. Campos, M. A. Stroschio, and K. W. Kim, *Semicond. Sci. Technol.* **7**, 60 (1992).
- ⁷V. B. Campos and S. Das Sarma, *Phys. Rev. B* **45**, 3898 (1992).
- ⁸M. A. Stroschio *et al.*, *Phys. Rev. B* **40**, 6428 (1989); *J. Superlatt. Microstruct.* **10**, 55 (1991).
- ⁹Q. P. Li and S. Das Sarma, *Phys. Rev. B* **43**, 11 768 (1991).
- ¹⁰S. Das Sarma *et al.*, *Phys. Rev. B* **41**, 3561 (1990), and references therein; see also S. Das Sarma, in *Hot Carriers in Semiconductor Nanostructures*, edited by J. Shah (Academic, New York, 1992), p. 53.
- ¹¹J. A. Kash, J. C. Tsang, and J. M. Hvam, *Phys. Rev. Lett.* **54**, 2151 (1985).